*Journal of Applied Mechanics and Technical Physics, Vol. 40, No. 4, 1999*

# OPTIMUM OVERTAKING COMPRESSION SHOCKS WITH RESTRICTIONS IMPOSED ON THE TOTAL FLOW-DEFLECTION ANGLE

**A. V. Omel'chenko and V. N. Uskov** UDC 533.6.011.72.

*The problem of optimization of gasdynamic variables behind a system of two steady oblique compression shocks with restrictions imposed on the flow-deflection angle is considered. The intervals of input parameters, in which this system turns out to be more effective than one shock, are determined. On the basis of an analysis of the system optimal for the static pressure, the physical meaning of the transition from one type of the reflected discontinuity to another is explained for the problem of interaction of overtaking oblique compression shocks.*

**1. Formulation of the Problem.** We consider a planar steady supersonic flow of a perfect inviscid gas passing through a system $S_2$, which consists of two oblique compression shocks aligned in one direction. The ratio of static pressures behind the $k$th shock ($p_k$) and ahead of it ($p_{k-1}$) determines the shock strength $J_k = p_k/p_{k-1}$ ($k = 1$ and 2). As shown, e.g., in [1], for fixed values of the ratio of specific heats $\gamma$ and the Mach number $\mathrm{M}_{k-1}$ ahead of the $k$th shock, the ratio $f_k/f_{k-1}$ of the values of all gasdynamic variables $f$ behind and ahead of the shock ($f_k$ and $f_{k-1}$, respectively) is uniquely determined by its strength. In particular, the relation between the Mach numbers on the shock is given by

$$\frac{\mu(\mathrm{M}_k)}{\mu(\mathrm{M}_{k-1})} = \frac{J_k + \varepsilon}{J_k(1 + \varepsilon J_k)}, \qquad \mu(\mathrm{M}) = (1+\varepsilon)\mathrm{M}^2 - \varepsilon, \qquad \varepsilon = \frac{\gamma - 1}{\gamma + 1}. \tag{1.1}$$

The angle $\beta_k$ of flow deflection by the shock is also uniquely expressed through the strength $J_k$ of the $k$th shock and the Mach number $\mathrm{M}_{k-1}$ ahead of it [1]:

$$\beta_k = \arctan\left[\sqrt{\frac{(1+\varepsilon)\mathrm{M}_{k-1}^2}{J_k + \varepsilon} - 1}\,\frac{(1-\varepsilon)(J_k - 1)}{(1+\varepsilon)\mathrm{M}_{k-1}^2 - (1-\varepsilon)(J_k - 1)}\right]. \tag{1.2}$$

It was shown in [1–3] that systems $S_2$ are often more effective than a single compression shock and allow one to increase the magnitude of the gasdynamic variable $f$ behind $S_2$ compared to the corresponding values of $f$ behind an isolated shock. In this case, the total flow-deflection angle in the system can far exceed the deflection angle on one shock. The latter hinders the use of such system in real technical devices [4]. On this basis, it seems to be an urgent matter to perform an analysis of the systems $S_2$ with the following additional geometric restriction imposed on the flow-deflection angle:

$$\beta_1 + \beta_2 = \beta_s = \text{const}. \tag{1.3}$$

The aim of this work is an optimization study of the system $S_2$ under restriction (1.3).

**2. The Domain of Existence of the System $S_2$.** For a two-shock system $S_2$ to exist, it is required that the flow behind the first shock remain supersonic. The latter holds if the strength $J_1$ of the first shock is within the range $[1, J_*(\mathrm{M})]$. Here $\mathrm{M} \equiv \mathrm{M}_0$ is the free-stream Mach number and $J_*(\mathrm{M})$ is the shock strength

Baltic State Technical University, St. Petersburg 198005. Translated from Prikladnaya Mekhanika i Tekhnicheskaya Fizika, Vol. 40, No. 4, pp. 99–108, July–August, 1999. Original article submitted June 3, 1997.

 0021-8944/99/4004-0638 $22.00 

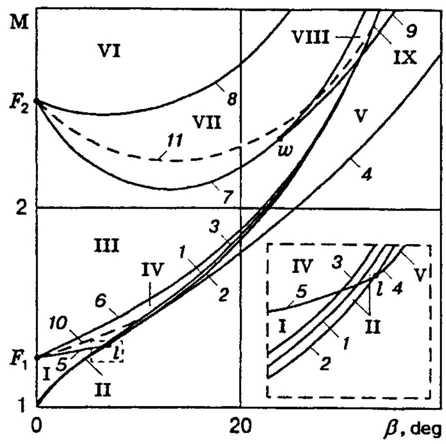


Fig. 1

given by (1.1) provided that $M_1 = 1$, which equals

$$J_* \frac{\mu - 1}{2\varepsilon} + \sqrt{\left(\frac{\mu - 1}{2\varepsilon}\right)^2 + \mu}. \tag{2.1}$$

The flow-deflection angle on such a shock is given by the formula

$$\beta_* = \arctan\left[\sqrt{\frac{J_* - 1}{1 + \varepsilon J_*}} \frac{(1 - \varepsilon)(J_* - 1)}{(J_* + \varepsilon) + (J_* - 1)}\right]. \tag{2.2}$$

The dependence $\beta_*(M)$ constructed using formulas (2.1) and (2.2) is shown in Fig. 1 (curve 1) (here and below, the calculation results for $\gamma = 1.4$ are presented). For $M \to \infty$, the function $\beta_*(M)$ monotonically tends to the largest possible flow-deflection angle $\beta_a$ on the shock:

$$\beta_a = \arctan \frac{1 - \varepsilon}{2\sqrt{\varepsilon}} \qquad (\beta_a = 45.585^\circ). \tag{2.3}$$

Restriction (1.3), together with (1.1) and (1.2), gives an implicit relation between the strengths $J_1$ and $J_2$ of the impinging waves. Indeed, setting $J_1$ from the interval $[1, J_*(M)]$, one can determine the flow-deflection angle $\beta_1$ on the first shock from (1.2), and then, using relation (1.3), determine the flow-deflection angle $\beta_2$ on the second shock.

It is well known (see, e.g., [5]) that there exist two different strengths of the shocks $[(J_2^{(\alpha)}$ and $J_2^{(\delta)})]$ which deflect the flow by one and the same angle $\beta_2$. The strength $J_2^{(\alpha)}$ (of the weak shock) lies within the interval $[1, J_l(M_1)]$ and the strength $J_2^{(\delta)}$ (of the strong shock) is within the interval $[J_l(M_1), J_m(M_1)]$. The quantity $J_m(M_1) = (1 + \varepsilon)M_1^2 - \varepsilon$ determines the strength of the normal shock in the flow with the Mach number $M_1$, and $J_l(M_1)$ corresponds to the shock, the deflection angle $\beta_l(M_1)$ on which attains its maximum at a given $M_1$. The functions $J_l(M)$ and $\beta_l(M)$ have the following form [5]:

$$J_l = \frac{\mu - (1 + \varepsilon)}{2\varepsilon} + \sqrt{\left(\frac{\mu - (1 + \varepsilon)}{2\varepsilon}\right)^2 + \frac{\mu(1 + 2\varepsilon) - 1}{\varepsilon}}; \tag{2.4}$$

$$\beta_l = \arctan\left[\sqrt{\frac{J_l - 1}{J_l + \varepsilon} \frac{(1 + \varepsilon) + (J_l + \varepsilon)}{1 + \varepsilon J_l}} \frac{(1 - \varepsilon)(J_l - 1)}{2(J_l + \varepsilon)}\right]. \tag{2.5}$$

The function $\beta_l(M)$ is plotted in Fig. 1 (curve 2). The function $\beta_l(M)$, as well as $\beta_*(M)$, tends to $\beta_a$ (2.3) as $M \to \infty$.

Generally, the second compression shock can be either weak or strong. Here, for definiteness sake, we assume it to be weak $[J_2 = J_2^{(\alpha)}]$. Then, the strength $J_2$ of the second shock and, hence, any gasdynamic variable behind it, is uniquely expressed through the strength of the first shock, $J_1$.

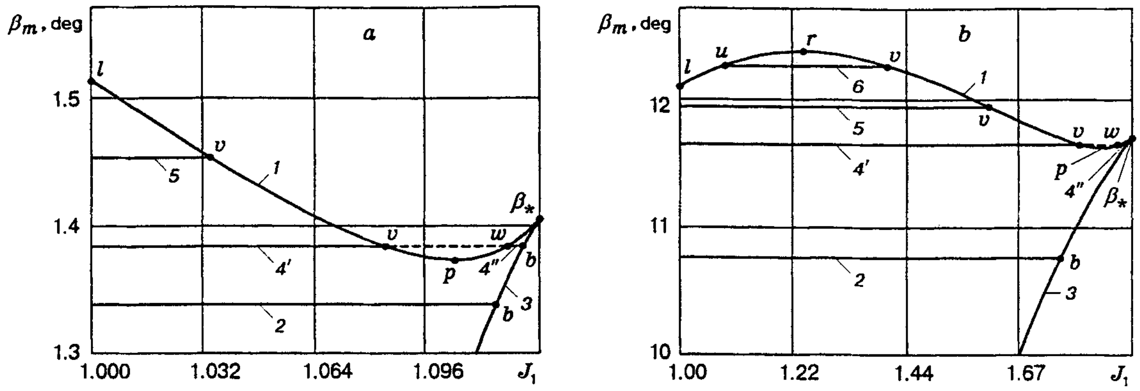


Fig. 2

The condition $J_1 \leqslant J_*(\mathrm{M})$ is necessary, but not sufficient for the existence of a system $S_2$ deflecting the flow by a preset angle $\beta_s > 0$. Indeed, the maximum flow-deflection angle in $S_2$ at a given $J_1$ is calculated from the formula [6]

$$\beta_m(J_1) = \beta_1(J_1) + \beta_l(\mathrm{M}_1). \tag{2.6}$$

The function $\beta_m(J_1)$ (curve 1 in Fig. 2) is defined on the interval $[1, J_*(\mathrm{M})]$. At the left end of the interval ($J_1 = 1$), the angle $\beta_m(J_1)$ coincides with the maximum angle $\beta_l(\mathrm{M})$ (2.5) of flow deflection by a single shock (point $l$ in Fig. 2). In the case $J_1 \to J_*$ (2.1), the Mach number $\mathrm{M}_1 \to 1$ and the limiting angle of flow deflection by the second shock $\beta_l(\mathrm{M}_1) \to 0$; hence, $\beta_m(J_1) \to \beta_*(\mathrm{M})$ (2.2) (point $\beta_*$ in Fig. 2).

As shown in [6] there are two characteristic ranges of Mach numbers separated by the value

$$\mathrm{M}_l = \frac{(J_g^2 - 1) + 2(J_g + \varepsilon)}{(J_g + \varepsilon) + (1 + \varepsilon)}, \quad J_g = \sqrt[3]{1 + \sqrt{1 - \frac{(1 + 2\varepsilon)^3}{27}}} + \sqrt[3]{1 - \sqrt{1 - \frac{(1 + 2\varepsilon)^3}{27}}} \tag{2.7}$$

($J_g = 1.606$ and $\mathrm{M}_l = 1.320$), in which the function $\beta_m(J_1)$ behaves differently. In the interval $\mathrm{M} \in [1, \mathrm{M}_l]$ (Fig. 2a, $\mathrm{M} = 1.1$), $\beta_m(J_1) < \beta_l(\mathrm{M})$ for each $J_1 \in [1, J_*]$ and this function has a minimum equal to $\beta_p(\mathrm{M})$ at a certain $J_1 = J_p(\mathrm{M})$ (point $p$ in Fig. 2). In the case $\mathrm{M} \in [\mathrm{M}_l, \infty)$ (Fig. 2b, $\mathrm{M} = 1.5$), there appears a region of $J_1$, where $\beta_m(J_1) > \beta_l(\mathrm{M})$. In this region, the function under study reaches its maximum value $\beta_m = \beta_r(\mathrm{M})$ at $J_1 = J_r(\mathrm{M})$ (point $r$ in Fig. 2 b). As a consequence, beginning from the Mach number $\mathrm{M}_l$, the maximum angle of flow deflection by two shocks $\beta_r(\mathrm{M})$ exceeds the limiting angle of flow deflection by a single shock $\beta_l(\mathrm{M})$.

According to the above-described behavior of the function $\beta_m(J_1)$, one can distinguish four types of domains of existence of the system $S_2$.

(1) For $\beta_s < \beta_p(\mathrm{M})$, the range of $J_1$ is a segment $[1, J_b]$ (straight line 2 in Fig. 2), where $J_b(\beta_s)$ is the strength of a single weak compression shock, which deflects the flow by a specified angle $\beta_s$ (curve 3 in Fig. 2). Indeed, for each value of $J_1$ taken from this range, the maximum angle of flow deflection by two shocks $\beta_m(J_1)$ (2.6) exceeds the preset value of $\beta_s$, and the system $S_2$ can deflect the flow by the angle $\beta_s$. If $J_1 > J_b$, then the angle of flow deflection by the first compression shock turns out to be larger than $\beta_s$, and, to deflect the flow by a preset angle, the second compression shock should change its direction, which is impossible in the framework of the chosen formulation of the problem.

(2) If $\beta_s \in [\beta_p(\mathrm{M}), \beta_*(\mathrm{M})]$, then, as shown in Fig. 2, straight line 4, which contains segments 4′ and 4″, intersects curve 1 at points $v$ and $w$ [the strengths $J_v$ and $J_w$ of the first shock in this case are determined as roots of the equation $\beta_m(J_1) = \beta_s$]. In the region $[J_v, J_w]$ (dashed segment of line 4), the system $S_2$ cannot deflect the flow by the angle $\beta_s$. Hence, for such $\beta_s$, the domain of existence of $S_2$ is subdivided into two subregions: $[1, J_v]$ and $[J_w, J_b]$ (segments 4′ and 4″ in Fig. 2).

(3) For the values of $\beta_s$ from the interval $[\beta_*(\mathrm{M}), \beta_l(\mathrm{M})]$, the subregion $[J_w, J_v]$ disappears, and the

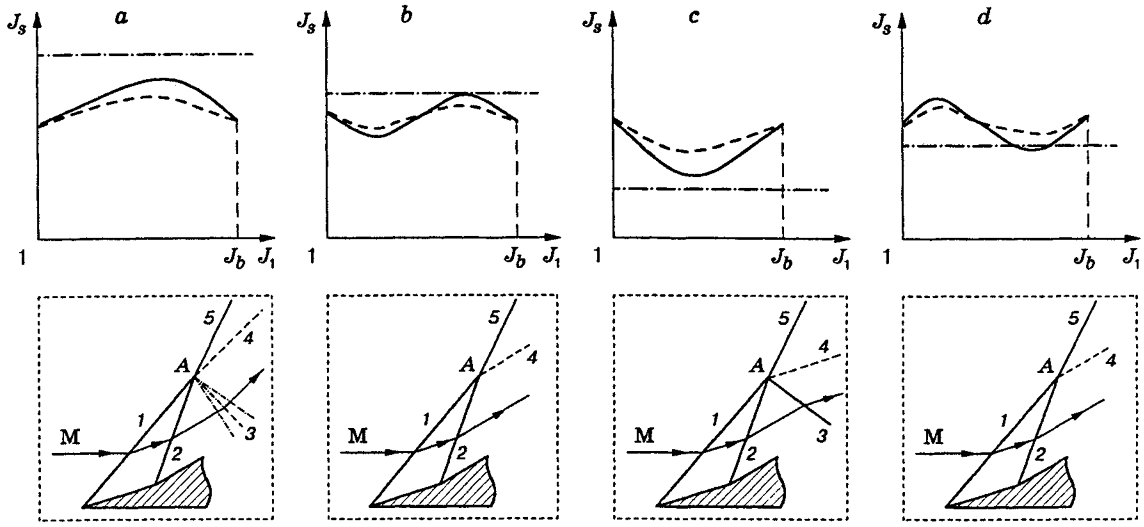


Fig. 3

system $S_2$ is defined on the segment $J_1 \in [1, J_v]$ (segment 5 in Fig. 2).

(4) For $M < M_l$ and $\beta_s > \beta_l(M)$, the system $S_2$ cannot exist. However, for $M > M_l$ and $\beta_s \in [\beta_l(M), \beta_r(M)]$, there is an interval $J_1 \in [J_u, J_v]$ (segment 6 in Fig. 2b) in which the system of two shocks can deflect the flow by the angle $\beta_s$.

The dependences $\beta_p(M)$ and $\beta_r(M)$, which give the minimum and maximum values of the function $\beta_m(J_1)$, were obtained in [6] (curves 3 and 4 in Fig. 1). As shown in Fig. 1, curves 1 and 3, which correspond to the functions $\beta_*(M)$ and $\beta_p(M)$, practically coincide at all values of M. By contrast, curve 4, which corresponds to the function $\beta_r(M)$ and issues from the point $l$ on curve 2, rapidly deviates from curve 2; already at $M = 2$ the maximum angle of flow deflection by two compression shocks exceeds the limiting angle of flow deflection by a single shock by 12%.

**3. Static-Pressure Behavior in the System.** As an example, we consider the behavior of the static pressure behind $S_2$. As shown in Sec. 2, restriction (1.3) allows one to uniquely determine the strength $J_2$ of the second shock from a given value of $J_1$. Hence, the dimensionless static pressure $J_s = p_2/p = J_1 J_2$ behind $S_2$ (the strength of the system) depends only on $J_1$.

Figure 3 shows the qualitative behavior of the function $J_s(J_1)$ in $S_2$. Depending on the values of the input parameters, the Mach number M and the angle $\beta_s$, one can distinguish nine characteristic domains on the plane $(\beta_s, M)$ (see Fig. 1), in which the function under study behaves differently.

In domains I, III, IV, VI, and VII (see Fig. 1) immediately adjacent to the vertical axis, the angle is $\beta_s < \beta_p(M)$, and, hence, the function $J_s(J_1)$ is defined on the entire segment $[1, J_b]$, where $J_b$ is the strength of a single shock deflecting the flow by a preset angle $\beta_s$. At the end points of this segment, the function assumes the same values equal to $J_b$: for $J_1 = 1$, the strength is $J_2 = J_s = J_b$; for $J_1 = J_b$, we have $J_2 = 1$, and, consequently, $J_s = J_b$.

The behavior of the function inside the interval $[1, J_b]$ substantially depends on the free-stream Mach number (solid curves in Fig. 3). For small M (domain I in Fig. 1 bounded by curves 3 and 5), the function $J_s(J_1)$ on the segment $(1, J_b)$ has only one extremum (maximum) at a certain $J_1 = J^{(1)}(M, \beta_s)$ (Fig. 3a). With increasing M, the position of the maximum shifts to the right end of the interval $(1, J_b)$. The transition to domain IV enclosed by curves 3, 5, and 6 (see Fig. 1) is accompanied by the appearance of a minimum $J_1 = J^{(2)}(M, \beta_s)$ at the left end of this interval (Fig. 3b), whereas the transition to domain III enclosed by curves 6 and 7 (see Fig. 1) is accompanied by vanishing of the maximum $J^{(1)}(M, \beta_s)$ (Fig. 3c). A further increase in the parameter M results in a nearly ideal repetition of the behavior of the function $J_s(J_1)$: with approaching domain VII located between curves 7 and 8 (see Fig. 1), the minimum shifts to the right, and the transition to domain VII gives rise to a maximum $J^{(1)}(\mathrm{M}, \beta_s)$ on the left end of the interval $[1, J_b]$ (Fig. 3d), whereas the transition to domain VI located above curve 8 (see Fig. 1) leads to disappearance of the minimum $J^{(2)}(\mathrm{M}, \beta_s)$ of the function under study. At large Mach numbers, the strength of the system on the segment $(1, J_b)$ again has only one extremum, a maximum (Fig. 3a).

As shown in Sec. 2, an increase in the parameter $\beta_s$ complicates the shape of the domain of definition of the function $J_s(J_1)$. As a consequence, its behavior becomes more complex as well. For example, upon approaching the right boundary of domain I (curve 3 in Fig. 1), the maximum $J^{(1)}(\mathrm{M}, \beta_s)$ tends to the point $J_p(\mathrm{M})$ of the minimum of the function $\beta_m(J_1)$. For $\beta_s = \beta_p(\mathrm{M})$ (i.e., on curve 3), these strengths coincides; in the case $\beta_s > \beta_p(\mathrm{M})$ the maximum falls in the segment $[J_v(\mathrm{M}), J_w(\mathrm{M})]$ where no solutions exist. The latter results in that, in domain II, whose boundaries are curves 2 and 3, the strength of the system is monotonic on each subinterval of its existence. A similar behavior is observed when passing from domain IV to domain II.

For $\mathrm{M} > \mathrm{M}_l$ (2.7), an additional domain of existence of the function under study appears (domain V in Fig. 1 enclosed by curves 2 and 4). In this domain, the function $J_s(J_1)$ behaves similarly as in domain II between curves 1 and 2.

An increase in $\beta_s$ at large M gives rise to an additional domain VIII (see Fig. 1) with three extrema of the function $J_s(J_1)$. This domain originates from the point $w$ and is enclosed by curves 7 and 9. For all points of domain III lying to the right of the point $w$, the transition to domain VII, where two extrema are observed, gives rise to an inflection point of the function on the lower boundary of domain VIII, which splits into two extrema (a maximum and a minimum) with increasing M. A further growth of M results in the displacement of the left minimum toward the lower end of the segment $[1, J_b]$ and its subsequent vanishing at the border with domain VII.

As shown in Fig. 1, at sufficiently large M, domain VIII intersects domains IV, II, and V. The intersection of domains VIII and IV gives rise to an additional domain IX with four extrema, which is bounded by curves 3 and 6. The intersection of domains VIII and II is accompanied by disappearance of the right maximum in a manner similar to that observed for small M, and the intersection of domains V and VIII by disappearance of the right subinterval of existence of the function $J_s(J_1)$.

Thus, on the plane $(\beta_s, M)$, there are several characteristic regions, in which the static pressure behind the system $S_2$ exhibits fundamental differences in its behavior. The aim of Sec. 4 is to find the boundaries of these domains and to determine the strength for which the function $J_s$ attains an extremum.

**4. Special Intensities and Mach Numbers.** The extremum values of the function $J_s(J_1)$ and the boundaries of the characteristic domains can be found using the Lagrange method of undetermined multipliers. For constant M and $\beta_s$, the Lagrange function

$$L = J_s + \lambda(\beta_1 + \beta_2 - \beta_s) \tag{4.1}$$

depends on three variables: wave strengths $J_1$ and $J_2$ and the Lagrangian multiplier $\lambda$.

Differentiating (4.1) with respect to $J_1$, $J_2$, and $\lambda$ and eliminating the Lagrangian multiplier $\lambda$, we can easily obtain a system of two equations, one of which is relation (1.3) and the other has the form .

$$\frac{\partial \beta_1}{\partial \Lambda_1} + \frac{\partial \beta_2}{\partial \Lambda_1} - \frac{\partial \beta_2}{\partial \Lambda_2} = 0. \tag{4.2}$$

As follows from the analysis performed in Sec. 3, the dependences $\beta_{\varphi_1}(\mathrm{M})$ and $\beta_{\varphi_2}(\mathrm{M})$ describing curves 5 and 7 in Fig. 1 are found from Eqs. (1.3) and (4.2) for $J_1 \to 1$. For the case $J_1 \to 1$, relation (4.2) reduces to a cubic equation in $\mathrm{M}^2$:

$$\begin{gathered}\sum_{n=0}^{3} A_n (\mathrm{M}^2)^n = 0, \qquad A_3 = J_2^2(1+\varepsilon)^2 - 4\varepsilon(J_2+\varepsilon)^2, \\ A_2 = 4\varepsilon(1-\varepsilon)(J_2+\varepsilon)(J_2^2-1) - 2(1-\varepsilon^2)J_2^2(J_2-1) - 4(1-2\varepsilon)(J_2+\varepsilon)^2, \\ A_1 = (1-\varepsilon)[4(1-2\varepsilon)(J_2^2-1)(J_2+\varepsilon) + 4(J_2+\varepsilon)^2 + (1-\varepsilon)J_2^2(J_2-1)^2], \\ A_0 = -4(1-\varepsilon)^2(J_2+\varepsilon)(J_2^2-1).\end{gathered} \tag{4.3}$$

Substituting the larger ($J_{\varphi_2}$) and medium ($J_{\varphi_1}$) roots of (4.3) into Eq. (1.3), which in the case $J_1 \to 1$ takes the form $\beta_{\varphi_i} = \beta_2(\mathrm{M}(J_{\varphi_i}), J_{\varphi_i})$ ($i = 1, 2$), one can obtain the desired dependences $\beta_{\varphi_1}(\mathrm{M})$ and $\beta_{\varphi_2}(\mathrm{M})$.

As shown in Fig. 1, curves 5 and 7 issue from the points $F_i$ located on the vertical axis. Substitution of $J_2 = 1$ into (4.3) yields the formula

$$\mathrm{M}_{F_i} = \sqrt{\frac{2}{5-3\gamma}[(3-\gamma) \mp \sqrt{\gamma^2-1}]} \qquad (i = 1, 2), \tag{4.4}$$

which gives the characteristic Mach numbers $\mathrm{M}_{F_i}$.

For increasing M, curve 7 tends to the maximum angle $\beta_a$ of flow deflection by a compression shock (2.3). In contrast to curve 7, curve 5 ends at the point $l$ on curve 2. It can be proved that the Mach number $\mathrm{M}_l$ corresponding to this point is given by formula (2.7).

As follows from the considerations in Sec. 3, to obtain the relations $\beta_{f_1}(\mathrm{M})$ and $\beta_{f_2}(\mathrm{M})$, which describe curves 6 and 8 in Fig. 1, one should pass to the limit $J_2 \to 1$ in Eqs. (1.3) and (4.2). In this case, from (4.2), the explicit analytical expressions

$$\begin{gathered}\mu_{f_i} = 1 + \varepsilon(\mathrm{M}_{f_i}^2 - 1) = A(B \pm C) \quad (i = 1, 2), \qquad A = \frac{1+\varepsilon J_1}{(1+\varepsilon)(J_1(1-3\varepsilon) - 4\varepsilon^2)}, \\ B = J_1(1 - 2\varepsilon - \varepsilon^2) - 2\varepsilon^2, \qquad C = 2\varepsilon\sqrt{\varepsilon(1+\varepsilon J_1)(J_1+\varepsilon)}\end{gathered} \tag{4.5}$$

follow which relate the Mach numbers $\mathrm{M}_{f_i}$ to the strength $J_1$ of the first shock. Substituting the resultant values of $\mathrm{M}_{f_i}$ into relation (1.3), which in the case $J_2 \to 1$ takes the form $\beta_{f_i} = \beta_1(\mathrm{M}_{f_i}(J_1), J_1)$ ($i = 1, 2$), one can obtain analytical expressions for curves 6 and 8.

Curves 6 and 8, as well as curves 5 and 7, issue from the points with the coordinates $(0, \mathrm{M}_{F_i})$ (4.4). For $\mathrm{M} \to \infty$, the dependence $\beta_{f_1}(\mathrm{M})$ tends to the value $\beta_a$ given by (2.3). The function $\beta_{f_2}(\mathrm{M})$, as M increases, asymptotically approaches the value

$$\beta_c = \arctan\frac{\sqrt{(1+\varepsilon)(1-3\varepsilon)}}{2\sqrt{\varepsilon}} \qquad (\beta_c = 43.100^\circ).$$

To describe curve 9 in Fig. 1, we should find the extrema of the implicit function $\mathrm{M}(J_1)$ given by Eqs. (1.3) and (4.2). As the calculations show, the minimum of the function implies the appearance of two additional extrema of the function $J_s(J_1)$.

Writing for $\mathrm{M}(J_1)$ the Lagrange function

$$\Phi = \mathrm{M} + \lambda_1(\beta_1 + \beta_2 - \beta_s) + \lambda_2\Big(\frac{\partial\beta_1}{\partial\Lambda_1} + \frac{\partial\beta_2}{\partial\Lambda_1} - \frac{\partial\beta_2}{\partial\Lambda_2}\Big),$$

differentiating it with respect to the variables $J_1$, $J_2$, $\lambda_1$, and $\lambda_2$, and eliminating the Lagrangian multipliers $\lambda_i$ ($i = 1. 2$), we obtain a system of three equations

$$\Psi = \frac{\partial\beta_1}{\partial\Lambda_1} + \frac{\partial\beta_2}{\partial\Lambda_1} - \frac{\partial\beta_2}{\partial\Lambda_2} = 0, \qquad \frac{\partial\Psi}{\partial\Lambda_1} - \frac{\partial\Psi}{\partial\Lambda_2} = 0, \qquad \beta_w = \beta_1 + \beta_2.$$

The first two equations permit determination of M and $J_2$ from a given value of $J_1$. The third equation allows one to determine the angle $\beta_w$ of flow deflection by the system of two compression shocks with strengths $J_1$ and $J_2(J_1)$. Varying the value of $J_1$ from unity to infinity, we can plot the dependence $\beta_w(\mathrm{M})$ (curve 9 in Fig. 1). The point $w$, from which curve 9 issues, can be found by solving the system for $J_1 \to 1$ ($\mathrm{M}_w = 2.282$ and $\beta_w = 22.563^\circ$).

**5. Interrelation between the Two-Shock System and the Compression Wave.** To explain the nonmonotonic behavior of the static pressure in the system $S_2$, we compare the behavior of the function $J_s(J_1)$ with the strengths $J_b$ and $J_c$ of the compression wave and an ordinary Prandtl–Meyer compression wave, respectively, which deflect the undisturbed flow by the same preset angle $\beta_s$.

Dot-and-dashed straight lines corresponding to the strength $J_c$ of the compression wave, which deflect the flow by the angle $\beta_s$, are plotted in Fig. 3 for various values of M. The dashed curves in Fig. 1 show the values of the parameters $\beta_s$ and M obtained in [7] for which $J_c = J_b$ (curves 10 and 11). As shown in [7], these curves issue from the points $F_i$ (4.4) and fall within domains IV and VII. At all points belonging to these domains and not belonging to curves 10 and 11, the strengths are not equal ($J_c \neq J_b$) (see Fig. 3b and d), but close in value. The difference between them increases upon going farther from curves 10 and 11. In domain III, the strength $J_c$ is far smaller than $J_b$ (Fig. 3c), and in domains I and VI it is much greater (Fig. 3a).

As noted above, in the case $\beta_s \leqslant \beta_p(\mathrm{M})$ (i.e., at the points belonging to domains I, III, IV, VI, and VII), the function $J_s(J_1)$ at the end points of the interval $[1, J_b]$ coincides with $J_b$. In domain III, the strength of the entire system exceeds $J_b$ for all $J_1 \in (1, J_b)$ (Fig. 3c) and has a maximum, whose value tends to the strength $J_c$ of the compression wave. In domains I and VI, the function $J_s(J_1)$ also has one extremum (minimum) on the segment $(1, J_b)$, whose value, again, tends to $J_c$ (Fig. 3a). Finally, in domains IV and VII, where $J_c$ and $J_b$ differ only slightly, the strength $J_s(J_1)$ of the system oscillates near its "equilibrium position," i.e., the strength $J_b$.

The above consideration shows that the system under study consisting of two compression shocks is a peculiar kind of a compression-wave model. The static pressure behind $S_2$, which coincides with the static pressure behind a solitary shock at the end points of the interval $[1, J_b]$, tends to the pressure behind an ordinary wave deflecting the flow by an equal angle $\beta_s$. The number of extrema of the function $J_s(J_1)$ and their type depend on the sign and value of the difference between $J_c$ and $J_b$.

**6. Physical Meaning of the Reflected Discontinuity in the Problem of Interaction between Overtaking Compression Shocks.** During regular interaction between overtaking compression shocks 1 and 2 (Fig. 3), there appear an outgoing resulting shock 5 and reflected discontinuity 3, as well as tangent discontinuity 4 situated in between them [8]. The reflected discontinuity can be either a rarefaction wave (Fig. 3 a) or a compression shock (Fig. 3c). In a specific case, this discontinuity is a weak discontinuity (Fig. 3b and d) and the structure arising in this process is a triple shock-wave configuration. The strengths of the outgoing (5) and reflected (3) discontinuities can be found from the conditions of equal static pressures and flow-deflection angles on both sides of tangent discontinuity 4, i.e., from the solution of the system

$$J_1 J_2 J_3 = J_5, \qquad \beta_1 + \beta_2 \pm \beta_3 = \beta_5.$$

Here $J_i$ ($i$ = 1, 2, 3, and 5) are the strengths of the corresponding discontinuities and $\beta_i$ are the angles of flow deflection on them. The plus at $\beta_3$ refers to a reflected rarefaction wave, and minus to a compression shock.

The comparison between the static pressure behind the compression shock, the compression wave, and the system $S_2$ under restriction (1.3) performed in Sec. 5 allows the following simple explanation for the appearance of a reflected discontinuity at the point where the overtaking compression shocks interact with one another.

First, we consider the case in which the compression-wave strength far exceeds the strength of the compression shock, which deflects the flow by an equal angle (domains I and VI in Fig. 1). As shown in Sec. 5, the static pressure behind the system of two overtaking shocks exceeds the static pressure on one shock. When such shocks interact with one another, a centered rarefaction wave must appear (Fig. 3a) which levels out the static pressure on tangent discontinuity 4. This wave, first, decreases the static pressure behind $S_2$, and, second, further deflects the flow by an angle greater than $\beta_s = \beta_1 + \beta_2$, thus increasing the angle $\beta_5$ of flow deflection on shock 5 from the interaction point $A$ and raising the static pressure behind this shock.

The opposite situation is observed for $J_b \gg J_c$ (domain III in Fig. 1). In this case, for an equal flow-deflection angle, the static pressure behind one shock exceeds the pressure behind the system $S_2$ consisting of two shocks. The reflected discontinuity 3 resulting from the interaction between the two shocks should be a compression shock (Fig. 3c). On the one hand, it increases the static pressure behind $S_2$; on the other hand, it decreases the static pressure behind shock 5 at the expense of a decrease in the flow-deflection angle $\beta_5$ on it compared to the angle $\beta_s$ of flow deflection in the system $S_2$.

Finally, in the situation where $J_b \approx J_c$ (domains IV and VII in Fig. 1), the function $J_s(J_1)$ can be either greater or smaller than $J_b$ (Fig. 3b and d). In the first case, the reflected discontinuity is a rarefaction wave, and, in the second, it is a compression shock. In both cases, its strength is close to unity. The exact equality $J_3 = 1$ is attained at a certain $J_1$ from the interval $(1, J_b)$, and corresponds to a triple shock-wave configuration (Fig. 3b). The boundaries $\beta_{\varphi_i}(\mathrm{M})$ and $\beta_{f_i}(\mathrm{M})$ of domains IV and VII [formulas (4.3) and (4.5)] are boundaries of the domains of existence of triple configurations [9, 10].

Thus, transition from domain I, in which $J_c > J_b$, to domain III, in which the reverse inequality holds, leads to a change of the type of not only the extremum of the function $J_s(J_1)$ in the system $S_2$, but also the reflected discontinuity during the interaction between overtaking compression shocks, and to the occurrence of domain IV where triple configurations are possible. In a similar manner, the change of the sign of the difference $J_c - J_b$ to the opposite upon going from domain III to domain VI is accompanied by the appearance of the second domain where triple configurations are possible (domain VII) and by the transition from the interaction with a reflected compression shock to the interaction with a reflected centered rarefaction wave.

**7. Additional Remarks.** (1) In Sec. 6, the interrelation between the problem of interaction of overtaking compression shocks and the problem of modeling the system $S_2$ under imposed restriction (1.3) were demonstrated for the case in which the point with the coordinates $(\beta_s, \mathrm{M})$ belongs to the domains immediately adjacent to the ordinate axis. As noted above, an increase in the parameter $\beta_s$ makes the domain of definition of the function $J_s(J_1)$ more complex and its behavior more intricate. An increase in $\beta_s$ in the problem of overtaking shocks is accompanied by the transition from regular to irregular interaction and by the appearance of regions where there is no solution of the problem of interest [5]. In this case, the boundaries of irregular interaction between the shocks and those of the domains where no solutions exist coincide with the boundaries of the characteristic regions plotted in Fig. 1 when performing an analysis of the system optimal from the viewpoint of the static pressure. Hence, two problems are interrelated for all values of M and $\beta_s$.

(2) The allowance for the shocks of the system $S_2$ in domains I, III, IV, VI, and VII does not change the qualitative behavior of the static pressure behind the system. The latter follows from Fig. 3a–d, where the dashed curves show the values of the function $J_s' = J_1 J_2 J_3$, which gives the dimensionless static pressure behind the reflected discontinuity 3. As shown in Fig. 3, the reflected discontinuity decreases the amplitude of oscillations of the function $J_s(J_1)$ around its "equilibrium position," the strength $J_b$, i.e., this discontinuity acts as a damper in the system $S_2$. On the other hand, this discontinuity does not change the phase of these oscillations, and, hence, it leaves unchanged both the boundaries of the nonmonotonic behavior of the function $J_s'(J_1)$ and the number of its extrema.

(3) Omel'chenko and Uskov [11, 12] found the boundaries of nonmonotonic behavior of the function $J_s(J_1)$ in the systems $S_2$ consisting of successively positioned compression shock and rarefaction wave [11], and rarefaction wave and compression shock [12]. The main feature distinguishing them from the system considered in this work is that the parameter $\beta_s$ in such systems can be both positive and negative. In the case $\beta_s > 0$, the boundaries of nonmonotonic behavior of the function $J_s(J_1)$ in the systems with a rarefaction wave coincide with the boundaries of nonmonotonic behavior of the static pressure in the two-shock system, i.e., they are described by the functions $\beta_{\varphi_i}(\mathrm{M})$ (4.3) and $\beta_{f_i}(\mathrm{M})$ (4.5). In Sec. 6, it has been established that these functions simultaneously serve as boundaries of the domains where the change of the type of the reflected discontinuity is observed in the problem of interaction between overtaking compression shocks. In the problems of interaction of a compression shock with a rarefaction wave, the boundaries of nonmonotonic behavior of the function $J_s(J_1)$ can be assumed to play the same role, i.e., they are boundaries of the domains where the type of the reflected discontinuity changes.

## REFERENCES


1. A. V. Omel'chenko and V. N. Uskov, "Optimal impact-wave systems," *Izv. Ross. Akad. Nauk, Mekh. Zhidk. Gaza*, No. 6, 118–126 (1995).
2. G. I. Petrov, *High-Velocity Aeromechanics and Space Research* [in Russian], Nauka, Moscow (1992).
3. R. German, *Supersonic Inlet Diffusers* [in Russian], Fizmatgiz, Moscow (1960).
4. G. N. Abramovich, *Applied Gasdynamics* [in Russian], Part 1, Nauka, Moscow (1991).
5. A. L. Adrianov, A. L. Starykh, and V. N. Uskov, *Interference of Steady Dasdynamic Discontinuities* [in Russian], Nauka, Novosibirsk (1995).

6. A. V. Omel'chenko and V. N. Uskov, "Maximal supersonic-flow deflection angles in impact-wave systems," *Izv. Ross. Akad. Nauk, Mekh. Zhidk. Gaza*, No. 3, 148–156 (1998).
7. A. V. Omel'chenko and V. N. Uskov, "Decay of a centered Prandtl–Meyer compression wave in a steady gas flow," *Prikl. Mekh. Tekh. Fiz.*, **39**, No. 3, 59–68 (1998).
8. G. S. Roslyakov, "Interaction between identically oriented planar shocks," in: *Numerical Methods in Gas Dynamics* [in Russian], Izd. Mosk. Univ., Moscow (1965), pp. 28–51.
9. V. Vust, "On the theory of branched compression shocks," in: *Gas Dynamics* [Russian translation], Izd. Inostr. Lit., Moscow (1950), pp. 131–143.
10. F. Vecken, "Limiting positions of fork-like compression shocks," *Mekhanika*, No. 4, 24–34 (1950).
11. A. V. Omel'chenko and U. V. Uskov, "Optimal impact-wave systems under restrictions on the total flow-deflection angle," *Izv. Ross. Akad. Nauk, Mekh. Zhidk. Gaza*, No. 2, 142–150 (1996).
12. A. V. Omel'chenko and U. V. Uskov, "An optimal shock-expansion system in a steady gas flow," *Prikl. Mekh. Tekh. Fiz.*, **38**, No. 2, 40–47 (1997).